N-27
61511
p. 30

NASA
Technical
Memorandum

NASA TM - 103561

NO-VENT FILL PRESSURIZATION TESTS USING A CRYOGEN SIMULANT

By G.R. Schmidt, R.W. Carrigan, J.E. Hahs,
D.A. Vaughan, and D.C. Foust

Propulsion Laboratory
Science and Engineering Directorate

December 1991

NASA
National Aeronautics and
Space Administration
George C. Marshall Space Flight Center

REPORT DOCUMENTATION PAGE

Form Approved
OMB No. 0704-0188

1. AGENCY USE ONLY *(Leave blank)*

2. REPORT DATE
December 1991

3. REPORT TYPE AND DATES COVERED
Technical Memorandum

4. TITLE AND SUBTITLE
No-Vent Fill Pressurization Tests Using a Cryogen Simulant

5. FUNDING NUMBERS

6. AUTHOR(S)
G.R. Schmidt, R.W. Carrigan, J.E. Hahs, D.A. Vaughan,*
and D.C. Foust*

7. PERFORMING ORGANIZATION NAME(S) AND ADDRESS(ES)
George C. Marshall Space Flight Center
Marshall Space Flight Center, Alabama 35812

8. PERFORMING ORGANIZATION REPORT NUMBER

9. SPONSORING/MONITORING AGENCY NAME(S) AND ADDRESS(ES)
National Aeronautics and Space Administration
Washington, DC 20546

10. SPONSORING/MONITORING AGENCY REPORT NUMBER
NASA TM-103561

11. SUPPLEMENTARY NOTES
Prepared by Propulsion Laboratory, Science and Engineering Directorate.

*Martin Marietta Space Systems, Huntsville, Alabama 35812

12a. DISTRIBUTION / AVAILABILITY STATEMENT
Unclassified – Unlimited

12b. DISTRIBUTION CODE

13. ABSTRACT *(Maximum 200 words)*

This report describes the results of an experimental program which investigated the performance of various no-vent fill techniques for tank-to-tank liquid transfer. The tests were performed using a cryogen simulant (Freon-114) and a test-bed consisting of a multiple tank/plumbing network that enabled investigations of a variety of different inlet flow and active mixing regimes. Several results and conclusions were drawn from the 26 transfer experiments comprising the program. Most notable was the significant improvement in fill performance (i.e., minimized fill time and maximized fill fraction) with increased agitation of the liquid surface. Another was the close correlation between measured condensation rates and those predicted by recent theories which express condensation as a function of turbulent eddy effects on the liquid surface. In most cases, test data exhibited strong agreement with an analytical model which accounts for tank heat transfer and thermodynamics in a 1-g environment.

14. SUBJECT TERMS
Cryogenic fluid, no-vent fill, tank pressurization, ground test, Freon-114, fluid management, low-g fluid transfer

15. NUMBER OF PAGES
27

16. PRICE CODE
NTIS

17. SECURITY CLASSIFICATION OF REPORT	18. SECURITY CLASSIFICATION OF THIS PAGE	19. SECURITY CLASSIFICATION OF ABSTRACT	20. LIMITATION OF ABSTRACT
Unclassified	Unclassified	Unclassified	Unclassified

TABLE OF CONTENTS

	Page
INTRODUCTION	1
OBJECTIVES	1
APPROACH	2
Test Article Design	2
Flow Regimes	4
Analysis	6
RESULTS	7
Bottom Fill Tests (Test Series 1)	7
Pressurant Collapse Test (Test Series 2)	7
Top Fill Tests (Test Series 3)	7
Active Mixing Tests (Test Series 4, 5, and 6)	9
ANALYSIS AND DISCUSSION	9
General Performance	9
Transient Behavior/FILL Model Evaluation	12
Evaluation of Condensation Theory	18
CONCLUSIONS	23
REFERENCES	25

LIST OF ILLUSTRATIONS

Figure	Title	Page
1.	Freon no-vent fill test article (FTA)	3
2.	Freon test article (FTA) schematic	4
3.	Fill regimes	5
4.	System-level comparison, test series 1 and 3	10
5.	System-level comparison, test series 3 and 6	11
6.	System-level comparison, test series 1, 4, and 5	12
7.	Inflow rate versus time	13
8.	Receiver tank volume versus time	13
9.	Interfacial mass transfer rate versus time	14
10.	Pressure ratio versus time	15
11.	Receiver tank pressure versus fill fraction	15
12.	Variation of FILL-calculated interfacial condensation rate	16
13.	Variation of liquid inflow temperature	17
14.	Variation of liquid inflow rate	17
15.	Variation of initial wall temperature	18
16.	Tank fluid temperature versus time	19
17.	Turbulence/condensation model for submerged horizontal jet	20
18.	Revised surface area geometry—top fill	21
19.	Turbulence/condensation model for quiessant top fill	21
20.	Comparison between top and bottom fill condensation behavior	23

TECHNICAL MEMORANDUM

NO-VENT FILL PRESSURIZATION TESTS USING A CRYOGEN SIMULANT

INTRODUCTION

No-vent fill is an important operation associated with the low-g transfer and resupply of cryogenic liquids and propellants. Much of the current technology work in this area has been focusing on development of computational models[1–5] to support the design of on-orbit storage facilities and space transportation propellant systems. Final validation of such tools will require data from cryogenic ground tests[6] and moderate to full-scale flight experiments[7] to evaluate the combined influence of cryogenic and microgravity fluid behavior. Until such tests are performed, simpler and smaller-scale ground experiments using fluids which emulate cryogen behavior are appealing for studying the fundamental mechanisms governing the process. In addition, small-scale tests can resolve many basic system-level issues which would otherwise increase the risk of costlier flight experiments.

One key system-level issue is design of the receiver tank's fill and mixing system. Besides minimizing fluid expended during prechill and conditioning, the main objectives are to enable fill without venting (i.e., independent of liquid/vapor orientation) and to maximize the quantity of liquid transferred within mission time and vessel pressure constraints. These are accomplished by mixing the bulk fluid and/or agitating the liquid surface, thus enhancing ullage collapse and condensation across the gas/liquid interface. Many types of fill and mixing concepts have been considered, some of which are quite costly. For future missions and applications, it is important to obtain data for evaluating and ranking different techniques.

Another issue relates to the computational tools needed for predictions and analysis of tank pressure histories, fill rates and general transient behavior. Such modeling requires a thorough accounting of the complex fluid mechanical, thermodynamic, and heat transfer phenomena occurring throughout the liquid, ullage, tank wall, and insulation. It also requires a means of characterizing mass transfer, primarily in the form of condensation, between the ullage and liquid. This has been difficult due to the general lack of understanding about the chief mechanisms responsible for condensation and evaporation. Although this topic has recently received much attention,[8 9] primarily in correlating the mass flux due to condensation with eddy effects and turbulence at the liquid surface, little has been done to experimentally validate the claims of these theories.

OBJECTIVES

The goal of the tests described in this report was to investigate as many basic no-vent fill issues as possible using a simple, subscale test-bed fabricated from inexpensive off-the-shelf hardware. Although the rudimentary design limited the precision of control over certain parameters (and the process in general), it did permit consideration of four experimental objectives.

The first was to compare several types of fill regimes and determine the most efficient method in terms of minimizing fill time and maximizing fill fraction. The fill techniques included passive and pump-assisted fills through various receiver tank inlet ports. An important aspect of this was to assess the benefits of different active mixing/circulation regimes, and compare these with less-sophisticated methods employing jet-induced agitation.

Another objective was to provide data (e.g., transient values of receiver tank pressure, temperature, fill rate, etc.) for evaluation and validation of FILL,[5] a tank thermodynamic model derived from the code used to analyze shuttle external tank (ET) heat transfer and pressurization. This was done not only to improve confidence in the model's predictive accuracy, but also to provide a benchmark before incorporating microgravity effects. Future plans include incorporation of algorithms which characterize surface area and interfacial mass transfer as a function of bond number, fill fraction, and inflow rate.

The third objective was to investigate the fundamental mechanisms governing condensation and ullage pressurant collapse. This involved calculating time-dependent condensation rates from test measurements and characterizing, with empirical approximations, fill level-dependent condensation flux in terms of representative dimensionless parameters. By applying several simplifying assumptions, the rate expressions for two fill methods were ratioed and compared over a range of conditions. This yielded unique insight into the behavior underlying different regimes and improved the understanding of how exposed surface area and interfacial turbulence interrelate during the fill process.

The fourth objective was to obtain data and experience that would guide follow-on ground testing with cryogens.

APPROACH

All experiments were performed using a subscale test-bed (i.e., Freon test article (FTA) (fig. 1)) and Freon-114 test fluid. Freon-114 was selected for several reasons. First, it is nontoxic and nonflammable, and, when the test article was originally built, it easily met safety and environmental criteria. Another feature that made Freon particularly appealing was its relatively low boiling point (~39 °F at 1 atm). Under typical ambient conditions, the fluid is in a saturated state and thus models the same general condensation/evaporation behavior as a cryogenic liquid. Freon-114 also has a relatively high vapor pressure which ensures a positive pressure differential with respect to the ambient environment and prevents leakage of contaminants into the system. Finally, because of Freon's compatibility with most water system components, the test facility could be built with standard plumbing hardware.

Test Article Design

A photograph and simplified schematic of the test article are shown in figures 1 and 2, respectively. The apparatus consisted of three insulated water heaters and a plumbing network affixed to a transportable pallet. Each test run involved flowing liquid from the transfer tank (T2) into the receiver tank (T3) through one or several different routing paths.

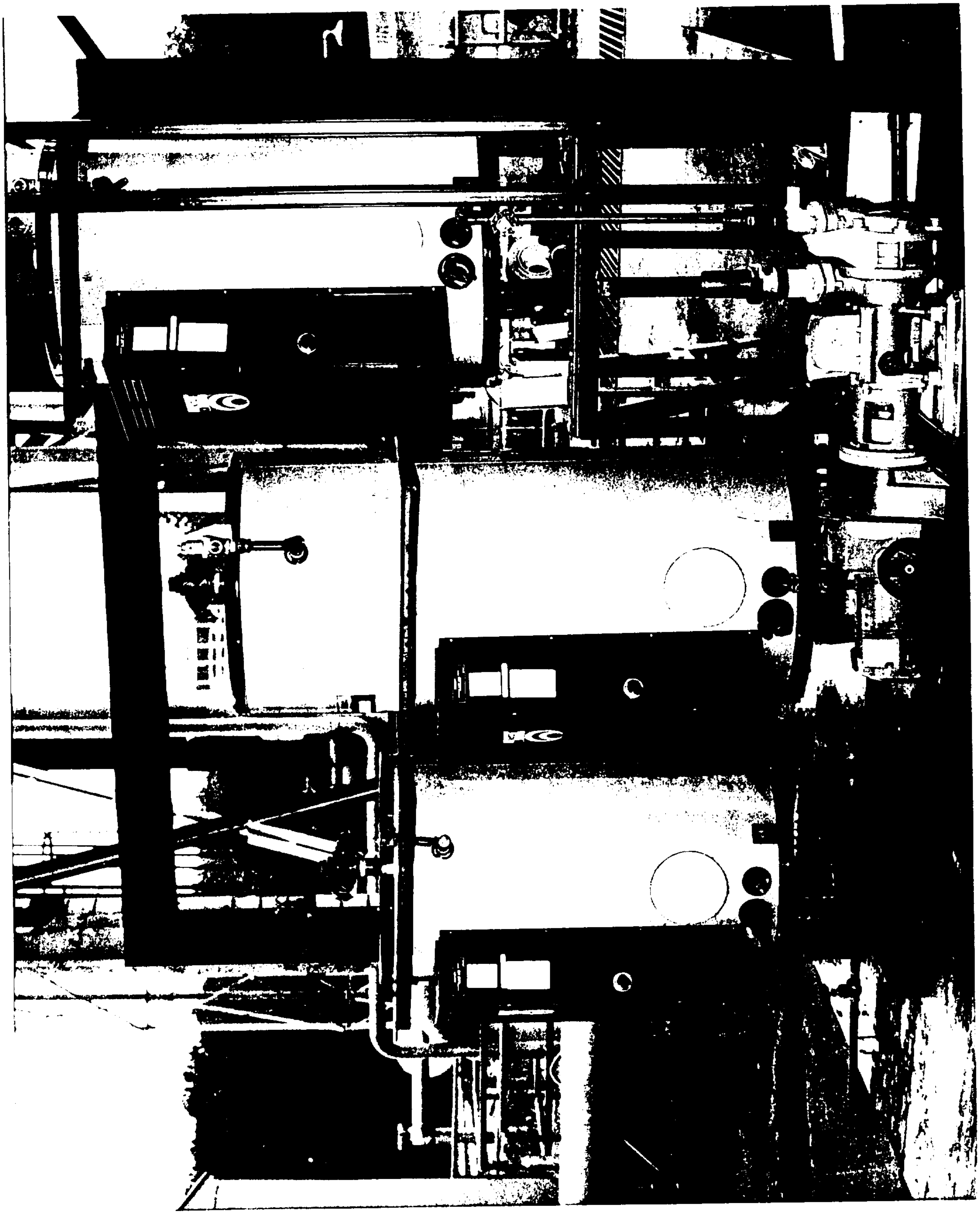

Figure 1. Freon no-vent fill test article (FTA).

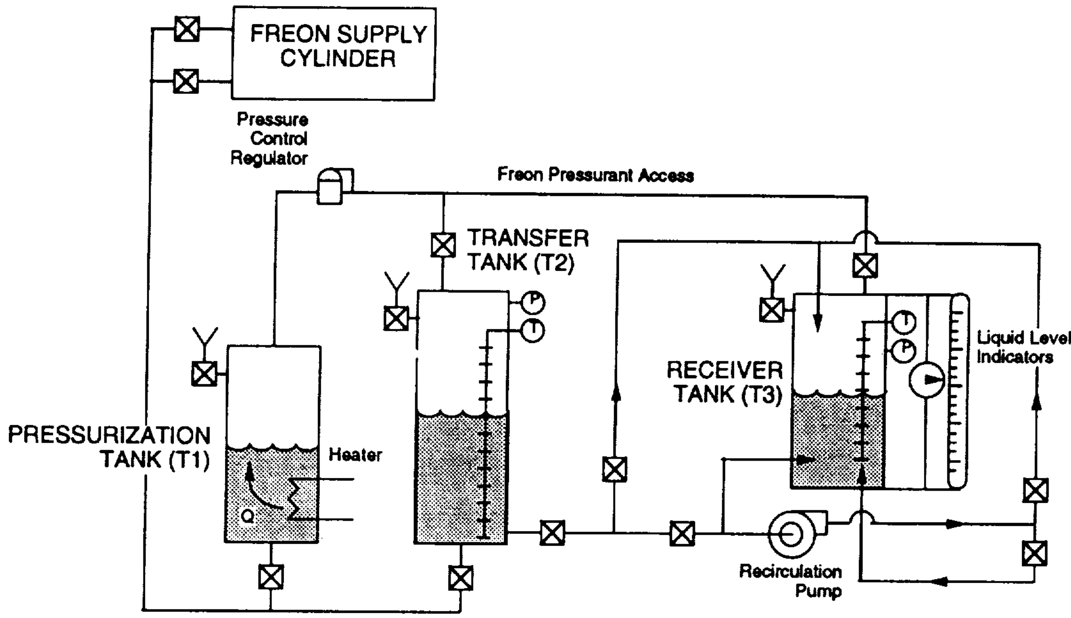

Figure 2. Freon test article (FTA) schematic.

The receiver tank had an internal diameter of 20.0 in and a maximum internal height/diameter ratio (z/D_{max}) of approximately 2.0. This yielded a volume of 50 gal and a tank mass/tank volume ratio of 5.0 lbm/ft^3. Inlet ports were located at the bottom and top of the tank. The bottom inlet was horizontal with respect to the liquid level and positioned approximately 2.0 in. above the base. The top inlet consisted of a 2.0-in diameter pipe pointing downward through the tank's upper dome. The pipe exit geometry was such that flow emanated at a conical half angle of approximately 25°.

The transfer tank served as a supply reservoir during the fill operation, and was larger (85 gal) to ensure complete fill of the receiver vessel. Liquid transfer was effected by autogenous pressurization of T2. Prior to each transfer, liquid in the 50-gal pressurization tank (T1) was vaporized and pressurized by energizing internal heating elements. During transfer, this vapor was routed through a regulator into the transfer tank ullage, thus maintaining a relatively constant back-pressure.

The principal data were obtained from thermocouples and pressure transducers located in each tank. Sight glasses were also used as a backup measure of fill level. Other important measurements included volumetric flowrate and recirculation pump speed.

Before initiating transfer, T3 was evacuated to the maximum extent possible. Because of the concave curvature of the base, it was impossible to rid the tank entirely of liquid without venting to the environment. To minimize Freon use, cost, and environmental impact, a small amount of liquid was left in the tank prior to each transfer. Thus, there was always some saturated vapor and liquid present at the beginning of each test.

Flow Regimes

The experimental program consisted of the following six series of tests:

(1) Quiescent bottom fill

(2) Pressurant collapse

(3) Quiescent top fill (enhanced fill)

(4) Bottom fill with active bottom recirculation

(5) Combined top and bottom fill with active bottom recirculation

(6) Combined top and bottom fill with active top recirculation.

Flow routings into the receiver tank for these tests are shown in figure 3. Series 1, 2 and 3 relied solely on the pressure difference between the transfer and receiver tank to effect liquid transfer, and were termed "quiescent" in that there was no externally applied mixing or circulation in the receiver vessel. The simplest of these was series 1 in which liquid from the transfer tank was injected into the receiver through the horizontal jet at the bottom of the tank. This regime best approximated a completely passive fill process and minimized inflow-induced agitation. It was also easiest to characterize analytically (because of the determinant geometry and predictable turbulence of the liquid surface), and was used as a reference for comparing other fill techniques.

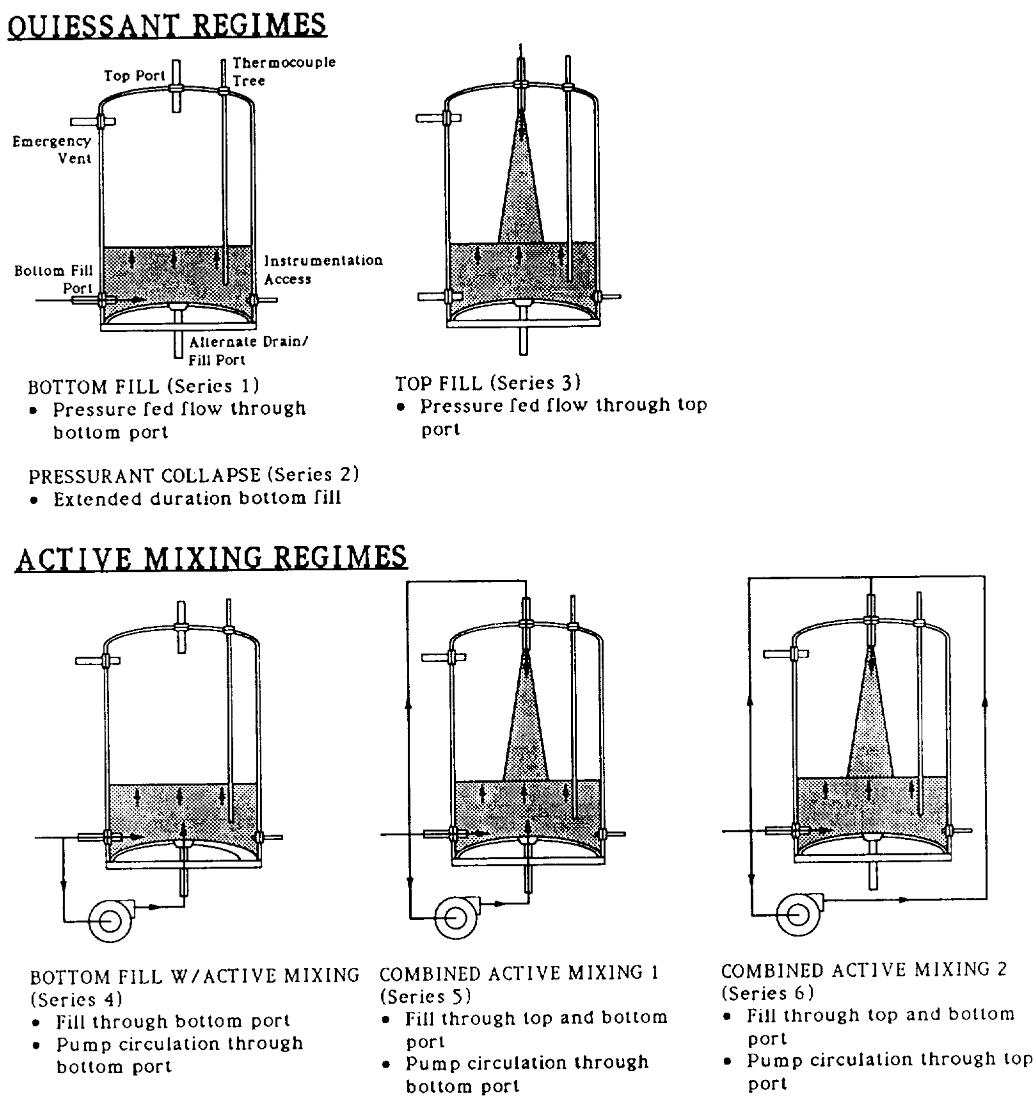

Figure 3. Fill regimes.

Test series 2 employed the same routing as series 1, and was performed solely to evaluate the influence of passive destratification on ullage pressure collapse. A much lower fill rate was obtained by reducing the pressure difference setting between the transfer and receiver tanks. In addition, data was recorded for a much longer duration (~2.0 h) in order to study how condensation rate varies in response to liquid conduction and destratification.

The third quiessant regime (series 3) entailed injection through a line located at the top of the receiver tank. Like the other two regimes, flow was effected solely by pressure difference. This test was included to assess the benefits of two condensation-enhancing effects: (1) the kinetic energy gained in falling to the bulk liquid surface, which tends to break up and increase liquid surface area, and (2) the increased surface area caused by exposure of the liquid jet to the ullage. The former effect promotes agitation of the exposed surface and thereby enhances condensation, while the latter one is particularly significant if the stream atomizes during descent.

Series 1 and 3 represented extremes of inflow-induced destratification and were useful in assessing the importance of inlet position. With bottom fill, incoming liquid collects around the entrance and suppresses disruption of the liquid surface. With the enhanced method, however, liquid enters as an impinging jet that continually agitates the liquid.

Test series 4, 5 and 6 differed from the first three in that active liquid mixing was employed within the receiver vessel. The choice of routings for these tests was somewhat arbitrary and almost entirely dictated by the limited number of available ports on the receiver vessel.

Series 4 represented the best direct comparison between the quiescent and active mixing regimes. These tests employed the same inflow routing as series 1. The only difference was the recirculation loop which extracted a small amount of inflow and pumped it into another port at the base of the tank. This loop ran outside the tank through a pump, and was intended to model the effects of a mixer on the bottom of the tank.

The other two active mixing regimes employed simultaneous fill through the top and bottom inlets. In series 5, the circulated liquid was injected through the receiver tank's bottom port, while, in series 6, the liquid was injected through the top port.

Analysis

Evaluation of test results involved three levels of analyses. The first entailed assessments of general system-level performance. There were a variety of parameters available for evaluating overall behavior, the most familiar being fill time, maximum fill level, receiver tank pressure ratio (final pressure/initial pressure) and average fill rate (maximum fill level/fill time). A comprehensive examination of all of these would have been difficult. Therefore, in order to provide a common basis for study, the time required to reach a fill fraction of 95 percent (Δt) was used as the principal system performance parameter. This eliminated fill level as a dependent variable and enabled comparisons based on transfer time versus pressure difference between the transfer and receiver tanks (ΔP).

The second type of analysis compared analytical model (i.e., FILL) predictions of transient state variables (i.e., temperature and pressure) with test data. This was required not only for evaluating the model's accuracy, but also for assessing the fill process' sensitivity to key parameters, such as fluid inlet temperature, liquid inflow rate, wall temperature, and condensation rate. Key data used in this analysis were plots illustrating pressure as a function of fill level (expressed as a percentage of tank volume).

The third type of analysis focused on evaluating current theories of condensation behavior. Condensation rate is virtually impossible to measure and must be calculated from test state property readings. This was done by reversing the FILL program logic and iteratively solving for temperature and condensation flux at each time step. By reconstructing condensation flux as a function of time, these data were correlated with measured fill levels to evaluate the functional relationship between flux and dimensionless liquid height (z/D). These rates were subsequently compared with predictions from universal submerged jet theory.[8 9]

RESULTS

A total of 25 transfers were conducted over the course of approximately 11 months (i.e., from Sept. 1989 to Aug. 1990). A summary of initial conditions and performance results is shown in table 1. The reference number indicates the chronological order in which each test was performed. Note that test -22 is not included, because it was actually a month-long monitoring operation and not a bonafide transfer experiment.

Bottom Fill Tests (Test Series 1)

Two of the 10 bottom fill transfers (i.e., -02 and -03) were discarded because the data acquisition time step setting was too long, and T3 filled too quickly to provide an accurate account of condensation rate. For this reason, a second series of tests was performed with a reduced acquisition time step and lower pressure difference. Also note that test -17 repeated the conditions of -08, which was later determined to contain inconsistent readings.

For the remaining seven "good" tests, the vapor supply pressure (i.e., T1 heater setting) and pressure drop across the regulator connecting T1 and T2 were varied to yield initial pressure differentials (ΔP) ranging from 17.3 to 39.0 psi. For the runs in which T3 was allowed to fill to 95 percent, fill times ranged from 63 s (for high ΔP) to 208 s (for low ΔP). Final pressure ratios (Pr) were also generally high and ranged from 1.54 to 1.83. The absolute pressures and temperatures in both tanks were different in each case due to seasonal variations in ambient temperature. In general, however, the fill time decreased and fill fraction increased with higher values of ΔP.

Pressurant Collapse Test (Test Series 2)

This test (test -09) was performed once with a low pressure difference of 4.1 psi. The transfer line was kept open for over 2 h. After a fairly rapid rise to a fill fraction of 60 percent in 225 s, the flowrate dropped off and stayed near zero for the remainder of the test.

Top Fill Tests (Test Series 3)

Three top fill tests were performed at pressure differentials of 12.0, 23.5 and 36.0 psi with corresponding Δt's of 144, 81 and 59 s. In all three cases, the receiver tank was filled to 95 percent of its capacity, and there was a progressive decrease in fill time with increased pressure differential. Also note that the pressure ratios ranged from 1.09 to 1.20 and were generally lower than those of other regimes.

Table 1. Results matrix.

RUNS			RUN CONDITIONS									PERFORMANCE RESULTS			
			Independent Parameters				Tank 2		Tank 3			Fill Performance			
TEST TYPE		Test Reference Number	T1 Heater Setting	Reg Press Drop (psi)	Pump Speed (rpm)	Circ Rate (gpm)	T2 Press (psid)	T2 Liq Temp (F)	T3 Press (psid)	D Press (psi) (P2-P3)	T3 Temp (F)	Fill Time (sec)	Final Fill Fraction	Initial Pr. Ratio*	Final Pr. Ratio*
QUIESSANT FILL TESTS	BOTTOM FILL (Series 1)	-01	1	10.0	N/A	N/A	23.8	88.0	5.9	17.9	58.5	184	95%	1.0	1.64
		-02	2	10.0	-	-	BAD	TEST	-	-	-	-	-	-	-
		-03	3	10.0	-	-	BAD	TEST	-	-	-	-	-	-	-
		-07	1	20.0	N/A	N/A	22.5	64.0	5.2	17.3	51.0	185	95%	1.0	1.66
		-08	3	15.0	N/A	N/A	44.0	114.	5.0	39.0	59.0	63	95%	1.0	1.83
		-17	3	15.0	N/A	N/A	47.5	83.5	23.2	24.3	87.0	208	95%	1.0	1.54
		-23	1	5.0	N/A	N/A	28.8	97.0	10.0	18.8	69.0	200	64%	1.0	1.63
		-24	1	10.0	N/A	N/A	27.2	93.0	9.1	18.1	78.0	201	53%	1.0	1.73
		-25	1	20.0	N/A	N/A	19.7	83.0	6.5	13.2	75.0	80	24%	1.0	1.50
		-26	1	20.0	N/A	N/A	21.0	84.0	9.2	11.8	78.0	61	33%	1.0	1.23
	TOP FILL (Series 3)	-04	1	15.0	N/A	N/A	20.5	83.0	8.5	12.0	71.0	144	95%	1.0	1.09
		-05	2	15.0	N/A	N/A	32.0	100.	8.5	23.5	62.0	81	95%	1.0	1.20
		-06	3	15.0	N/A	N/A	54.0	120.	18.0	36.0	74.0	59	95%	1.0	1.10
	PRESS COLL (2)	-09	1	-	N/A	N/A	19.6	67.0	15.5	4.1	75.0	225	60%	1.0	1.13
ACTIVE MIXING TESTS	BOTTOM w/ BOTTOM INJECTION (Series 4)	-11	1	15.0	1025	10.4	25.3	67.5	13.2	12.1	70.0	251	95%	1.0	1.27
		-14	1	15.0	1570	15.7	28.2	86.0	26.5	1.7	92.0	617	95%	1.0	0.99
		-19	1	15.0	2200	21.0	27.0	80.5	13.0	14.0	82.0	272	95%	1.0	1.27
	COMBINED w/ BOTTOM INJECTION (Series 5)	-12	1	15.0	1020	10.3	28.5	82.0	12.2	16.3	70.0	200	95%	1.0	1.44
		-15	1	15.0	-	-	BAD	TEST	-	-	-	-	-	-	-
		-16	1	15.0	1570	15.6	25.7	81.0	18.7	7.0	82.0	600	94%	1.0	1.14
		-20	1	15.0	-	-	BAD	TEST	-	-	-	-	-	-	-
		-21	1	15.0	2200	21.6	29.3	73.0	6.0	23.3	75.0	130	95%	1.0	1.64
	COMBINED w/ TOP INJECTION (Series 6)	-10	1	15.0	1025	11.0	21.5	62.0	6.5	15.0	63.5	127	95%	1.0	1.18
		-13	1	15.0	1570	16.5	27.5	81.5	20.5	7.0	87.5	157	95%	1.0	0.94
		-18	1	15.0	2200	20.0	28.0	75.0	14.0	14.0	77.0	123	90%	1.0	1.12

* Where Pr. Ratio equals the current receiver tank ullage pressure over the initial receiver tank ullage pressure.

Active Mixing Tests (Test Series 4, 5 and 6)

Series 4 (bottom fill with bottom recirculation) and 6 tests (combined top and bottom fill with top recirculation) were each performed three times, while series 5 tests (combined top and bottom fill with bottom recirculation) were conducted five times. During one of the runs, test -15, a pressure transducer failed, and test -16 was performed to repeat the conditions. In addition, test -20 was prematurely terminated due to inclement weather, and repeated with test -21. In all cases the same back pressure and regulator pressure drop were used. The only parameter that was intentionally varied in each series was pump speed which was set at increments of 1,030, 1,570 and 2,200 r/m.

The runs comprising test series 4 were conducted with ΔP's of 1.7, 12.1, and 14.0 psi yielding fill times of 617, 251, and 272 s, respectively. The higher pressure tests had lower fill times as expected and moderate pressure ratios (1.27) while the lower pressure test had a significantly higher fill time but lower pressure ratio of 0.99.

The runs comprising test series 6 were performed with ΔP's of 7.0, 14.0, and 15.0 psi resulting in fill times of 157, 123 and 127 s, respectively. The pressure ratios were also low at 0.94, 1.12, and 1.18.

The "good" runs comprising series 5 had driving pressures of 7.0, 16.3, and 23.3 psi yielding fill times of 600, 200, and 130 s and pressure ratios ranging from 1.14 to 1.64. This data closely resembled the bottom fill with active mixing (series 4) in that fill time was very sensitive to the driving pressure difference.

ANALYSIS AND DISCUSSION

General Performance

Figure 4 shows a plot of fill time (Δt) versus pressure difference (ΔP) for the quiessant bottom and top (enhanced) fill regimes (i.e., test series 1 and 3, respectively). A least-squares linear fit of the data is also shown to better illustrate comparative performance. It is obvious that the enhanced method is more efficient in terms of reducing fill time for a given ΔP. Table 1 also shows that the top fill regime yields a lower overall pressure rise in the receiver tank.

The best explanation for these lower transfer times and pressure ratios is the increased condensation encountered when filling through the top of the tank. Even though the regime is termed "quiescent," it is highly active in terms of promoting mass and heat transfer between the liquid and vapor. First, the ullage is cooled by the incoming fluid, thereby enhancing ullage pressure collapse. Secondly, when the fluid first enters the tank, a large amount of surface breakup occurs as the jet splashes against the bottom and side. This results in greater mixing and heat transfer between the gas and the liquid, and enhances ullage collapse relative to the bottom fill method. Third, as the liquid level increases a circulatory pattern is established which strongly affects surface turbulence. Sustaining strong circulation during the fill process, as in the case of top fill, increases condensation rate, and suppresses pressure rise. This is contrary to the bottom fill where circulation strength decreases as more liquid enters the tank.

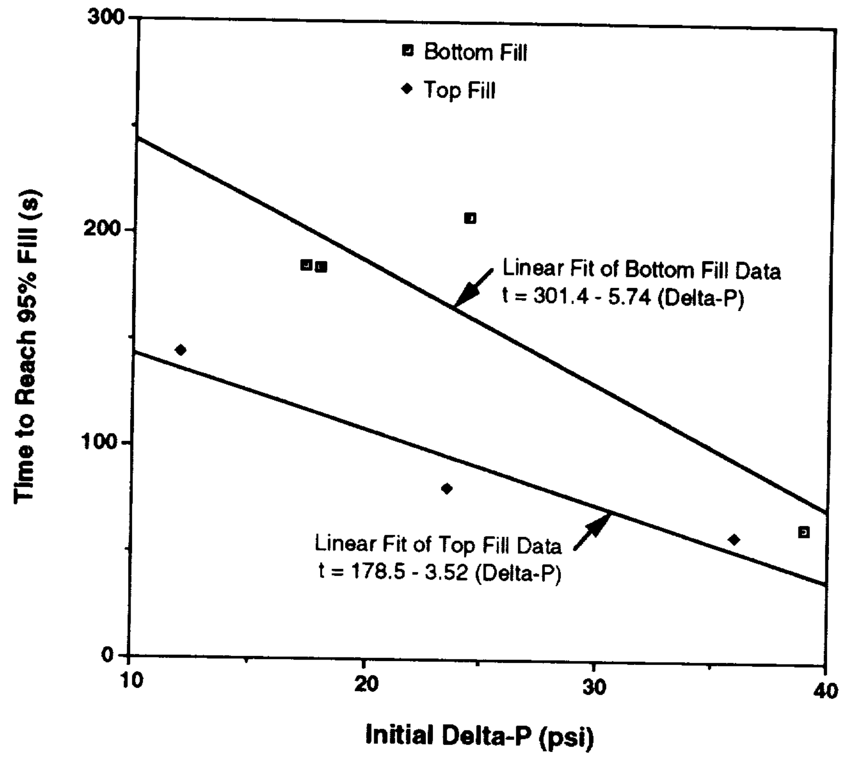

Figure 4. System-level comparison, test series 1 and 3.

The effect of active mixing is best evaluated by directly comparing the quiescent and active mixing regimes which are most similar in terms of inlet flow pattern. Figure 5 shows such a comparison between test series 3 and 6 which applies the same performance basis as before, namely Δt versus ΔP. The main difference between the two regimes is that, with the active mixing case, liquid feeds through both the top and bottom ports. In addition, the fluid transferred through the bottom is split and circulated through the pump into the top of the tank. The least-squares approximation in figure 5 indicates that fill times for the two regimes are essentially the same, considering experimental error and the limited number of available data points. One explanation for the negligible difference is that with series 6 the circulation pump draws off almost all of the pressure-fed flow and injects it through the top port. Thus, the active mixing test actually duplicates the same flow regime as the top fill case. Most importantly, it means that the full benefit of the pump cannot be realized because the flowrate is limited by pressure difference between the tanks.

No definitive conclusion pertaining to active mixing performance can be drawn from these results—at least with regards to actual space-based applications. In such an application, the circulation loop would extract bulk fluid from the tank, and would function independently of the transfer process. Thus mixing and destratification of tank contents could be performed at any time. In the FTA active mixing tests, the pump merely altered the routing of entering fluid and did not re-circulate the bulk contents per se.

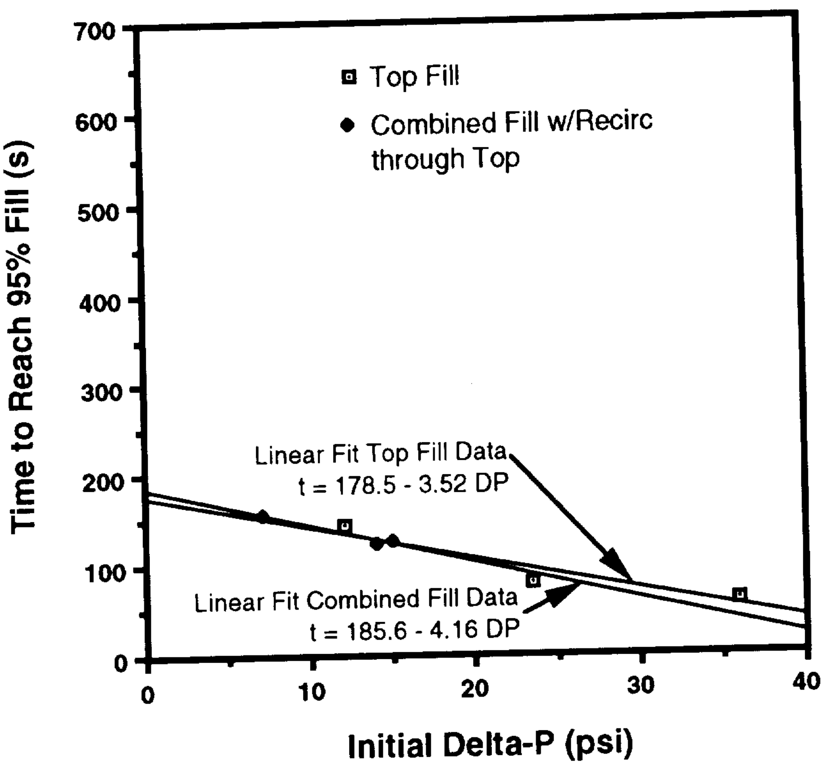

Figure 5. System-level comparison, test series 3 and 6.

A comparison between the bottom fill regime (test series 1) and active mixing tests employing bottom fill injection (test series 4 and 5) is shown in figure 6. Contrary to expectations, the behavior of the two active mixing regimes is very similar. Both show high transfer times at low ΔP's and performance comparable to the quiessant regime at higher ΔP's. Although the trends in figure 6 are rather crude and based on limited data, the discrepancy in behavior may be attributed to the limiting behavior of the pump. With active mixing, the pump draws off most of the flow and re-injects it into the bottom of the tank. At lower ΔP's the pump actually limits the rate of transfer and decreases fill rate of the tank, and the quiescent mode is superior. At higher ΔP's, the pump augments agitation and tends to improve performance. This conclusion, however, is rather tenuous and cannot be readily derived from the curve fits. The results at low ΔP's could be spurious in which case the trends of these active mixing tests may be very similar to those of series 6.

Lower pressure ratio is the only performance criteria in which series 4 and 5 were clearly superior to the quiescent bottom fill. This indicates that mixing, even with the impractical pumping routings, did enhance condensation.

From a systems standpoint, the top fill method appears to be the most efficient transfer technique over all. Test series 3 consistently yielded the lowest transfer times and pressure ratios of all fill methods tested. This result is significant from a design viewpoint. First, it suggests agitation as the best way for promoting mixing and ullage collapse. This supports use of a fairly simple inlet pipe arrangement rather than an exotic spray/atomization system. Second, the lower pressure ratios obtained with an agitated regime reduce tank design pressures, thus decreasing tank launch weight and cost. In addition, the plumbing and control systems for such a regime are far simpler and weigh

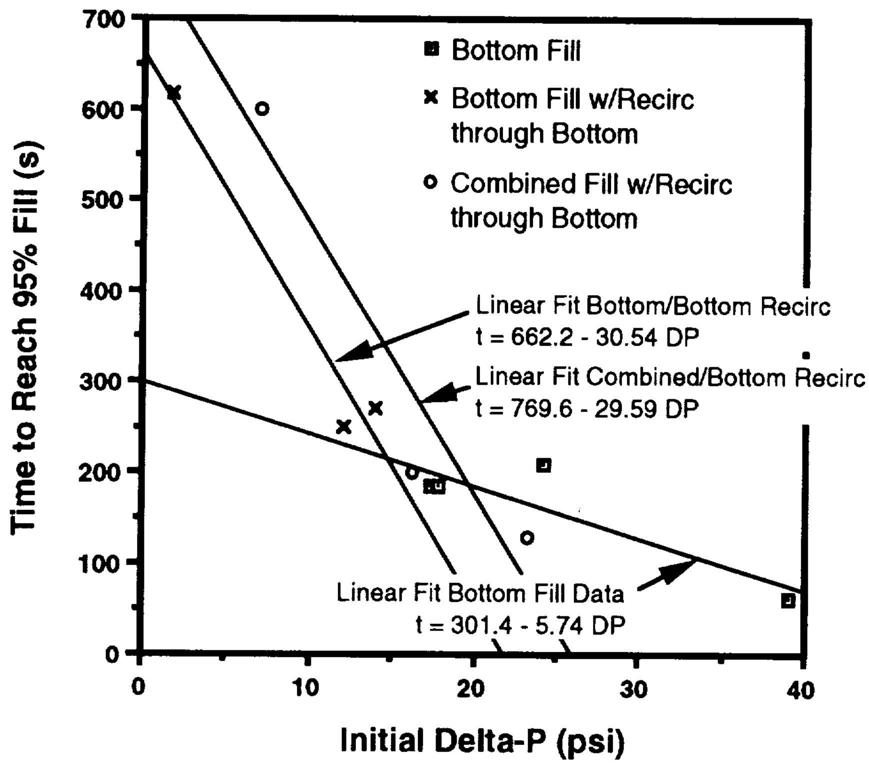

Figure 6. System-level comparison, test series 1, 4, and 5.

considerably less than a more sophisticated system. Third, the lower pressure difference lowers inlet flow impedance and decreases the total energy required to effect transfer.

Transient Behavior/FILL Model Evaluation

Test data consisted primarily of transient state properties and variables, and generally fell into three categories. The first consisted of sensor measurements and readings, such as flowrate and pressure. This type is illustrated in figure 7 which shows transient flowrate between T2 and T3 for a quiessant bottom fill (-17) and top fill (-04) test. The second category consisted of parameters calculated in real-time from test readings, such as fill levels and volumetric fractions. An example is shown in figure 8 which shows fill fraction calculated from pressure transducer measurements (hydrostatic head difference for liquid level) and an algorithm relating hydrostatic head to liquid height. The last type of data was similar to the second category but required more extensive calculations upon completion of testing. The best example (fig. 9) was interfacial mass transfer rate which was calculated from measured pressures, temperatures and surface area algorithms using the FILL model.

The comparative performance trends between test -04 and -17 (figs. 7 to 9) generally held true for all quiessant regimes. In most cases, series 3 tests exhibited higher inflow rates over the course of the fill process. Another notable difference was the consistently lower transient pressure rise for the top fill method. This is illustrated in figure 10 which shows receiver tank pressure (normalized with respect to initial pressure) as a function of time. In the bottom fill test, receiver tank pressure increased by 80 percent during the first 60 s of the transfer. For the top fill regime,

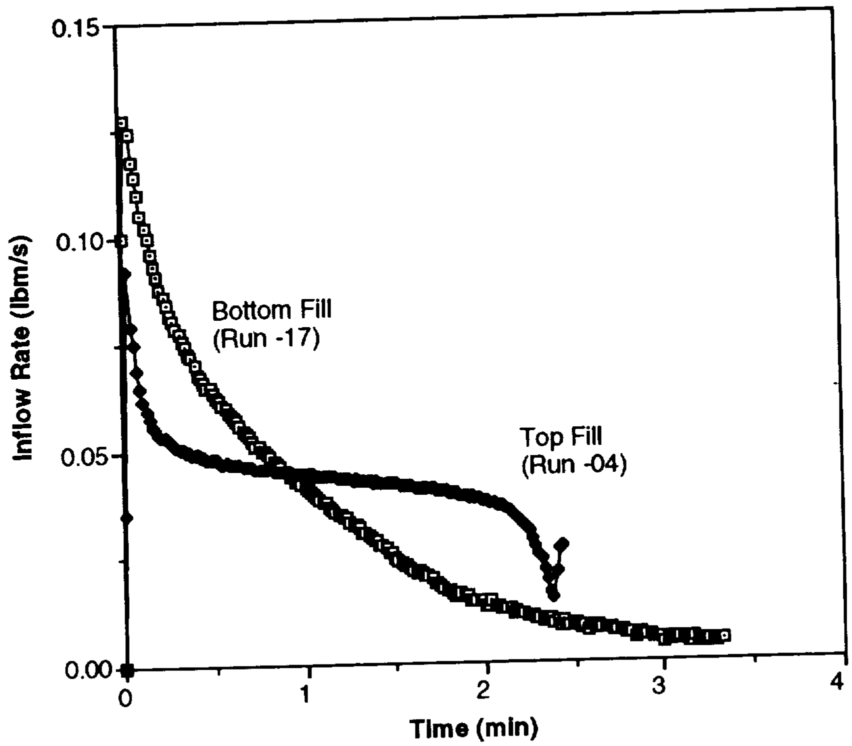

Figure 7. Inflow rate versus time.

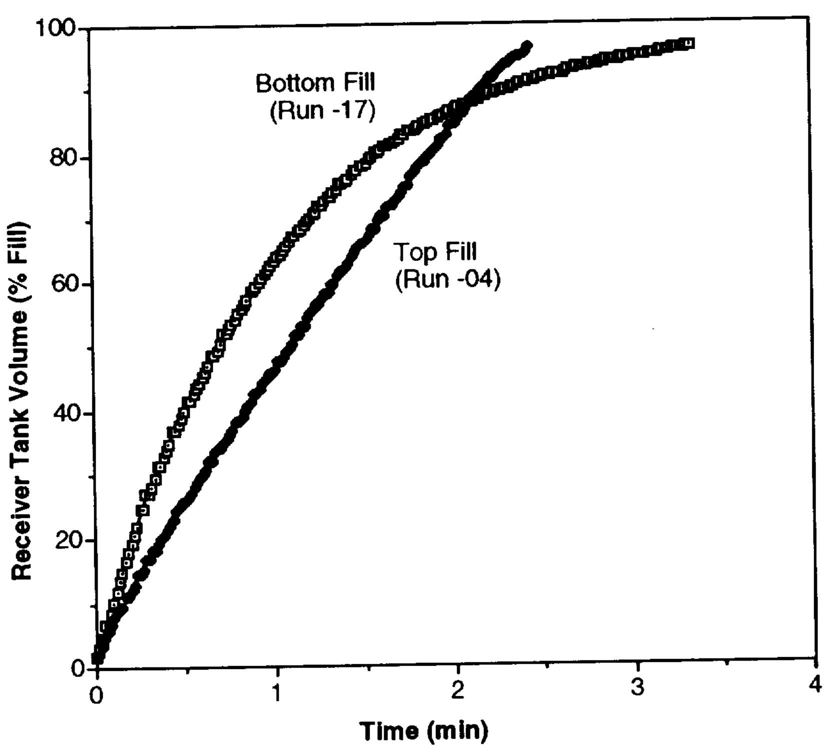

Figure 8. Receiver tank volume versus time.

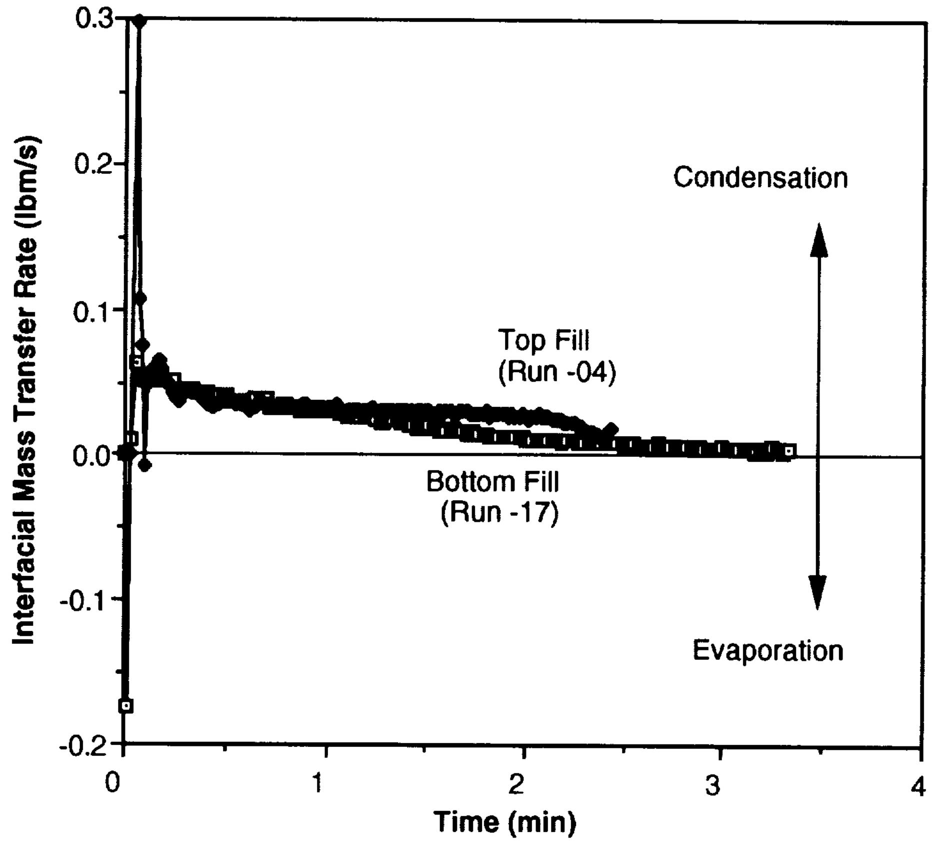

Figure 9. Interfacial mass transfer rate versus time.

however, pressure rose by only 10 percent. This difference, coupled with the reduced transfer times, indicates that the top fill regime was much more effective in enhancing ullage collapse and promoting condensation over the process. For this particular combination, the top fill reduced pressure rise by 39 percent, a marked improvement over the submerged jet fill.

Transient test measurements were also used to evaluate the FILL model's predictive accuracy, check its theoretical and empirical constitutive relationships, and validate its use for ground fill analysis. This was useful not only for verifying the model's accuracy but also for assessing the no-vent fill process' sensitivity to key parameters, namely fluid inlet temperature, liquid inflow rate, wall temperature, and condensation rate.

Figure 11 shows a plot of receiver tank pressure versus fill fraction from an FTA bottom fill test in which the average flowrate and fluid inlet temperature were held at 39.5 g/m and 516 R, respectively. Initially, the tank pressure is lower than the fluid's saturation pressure. This causes boiling and a sharp pressure rise as liquid first enters the tank. Boiling continues for only a few seconds until the tank pressurizes to a value greater than the liquid's saturation pressure. After this, the pressure rises slowly until the tank is approximately 80-percent full and then begins to increase at a higher rate. Probable causes for this sharp increase are the reduction in interfacial area as liquid fills the tank's top-dome section and the decrease in the condensation rate resulting from higher *z/D*.

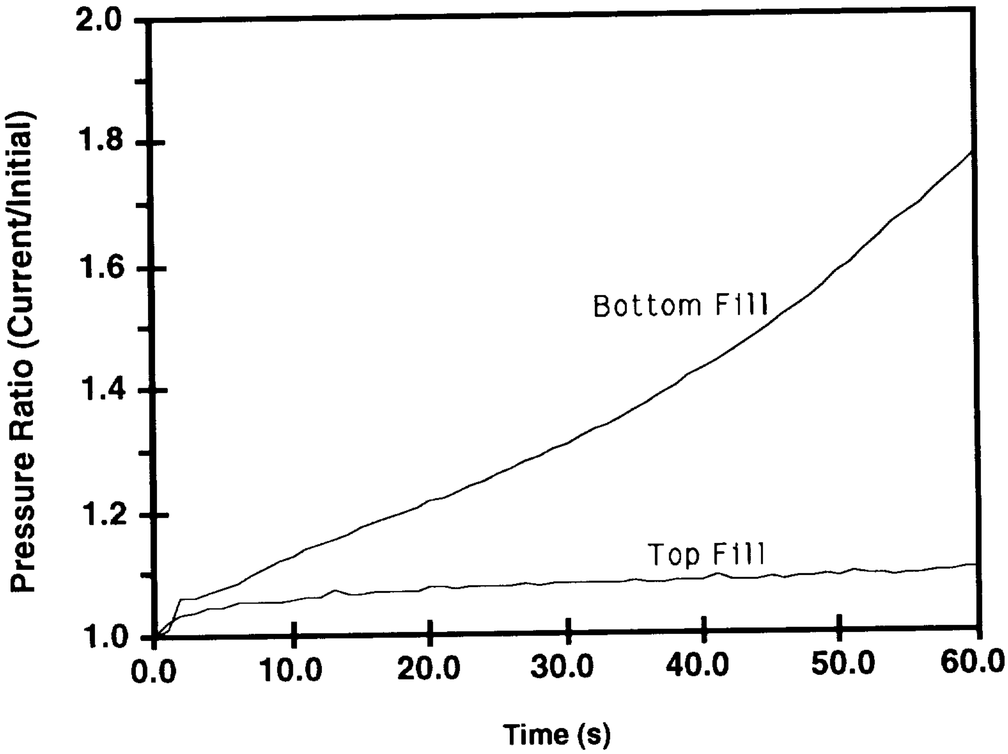

Figure 10. Pressure ratio versus time.

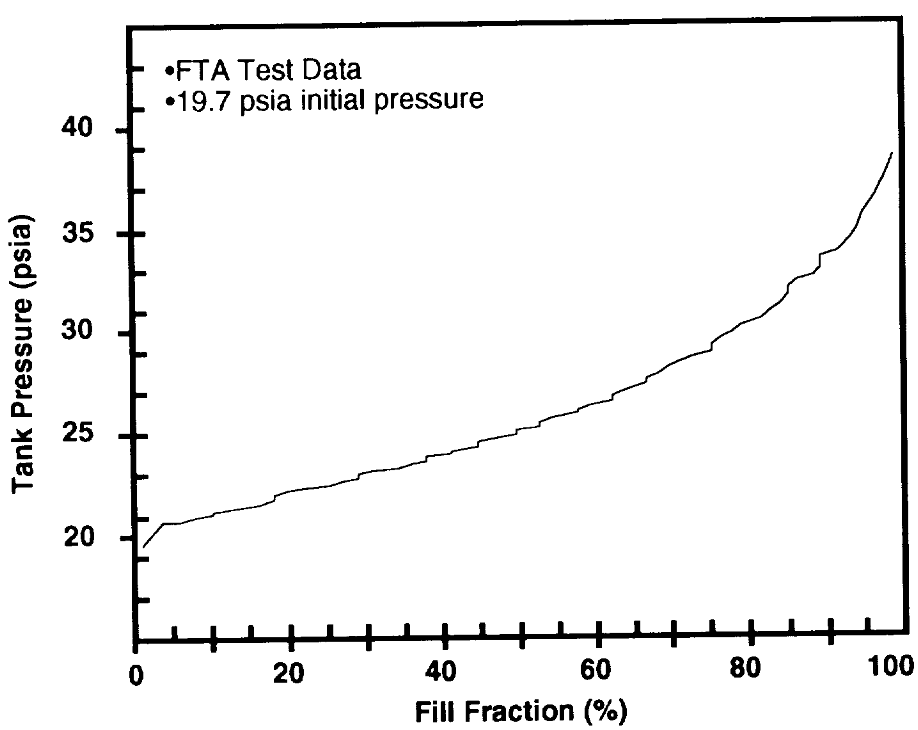

Figure 11. Receiver tank pressure versus fill fraction.

The control of FTA test conditions was somewhat limited due to its outdoor location and exposure to the environment. This made a strict comparison between FILL and FTA results rather difficult. To accommodate the uncertainty in test conditions, FILL pressure transients were generated in a parametric form over a range of parameter values. Liquid inflow rate and condensation rate were varied 20 percent from their nominal values. Liquid inlet temperature was varied by 4 R about a mean value of 519 R, while the initial tank temperature was varied by 40 R about a mean value of 550 R. Plots illustrating the sensitivity of pressure versus fill level (expressed as a percentage of the tank's volume) to these variations are shown in figures 12 through 15. Note that in figures 12 and 13 the pressure trace in figure 11 is overlayed on each graph.

The notable differences in pressure transients in figures 12 and 13 indicate that condensation rate and liquid inlet temperature have the greatest influence on tank pressure. Surprisingly, the effect of inflow rate, as shown in figure 14, is relatively minor. This can be explained by the nature of the constitutive relationship which expresses condensation rate as linearly proportional to liquid inflow rate. Consequently, compressive effects, which are expected to increase with higher flowrates, are offset by a corresponding increase in condensation.

The effect of wall temperature on ullage pressure is shown in figure 15. The relationship between the different traces indicates that wall temperature, at least for the FTA tests, does not play a critical role during the initial fill period. However, once the tank becomes approximately 50-percent full, wall temperature begins to play an important role.

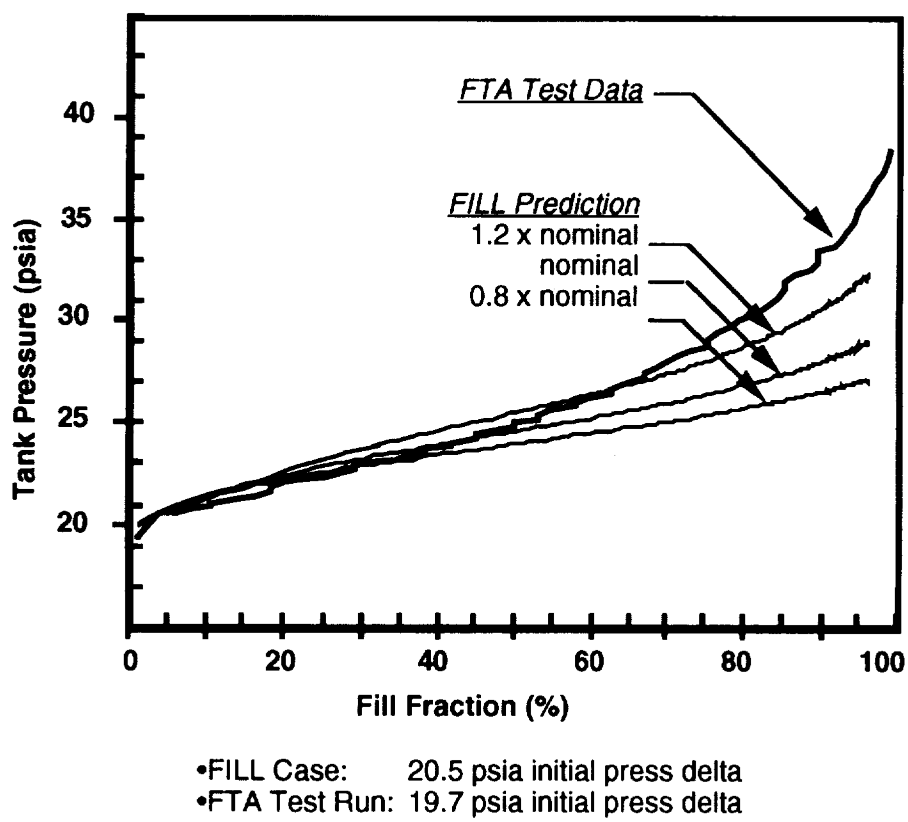

Figure 12. Variation of FILL-calculated interfacial condensation rate.

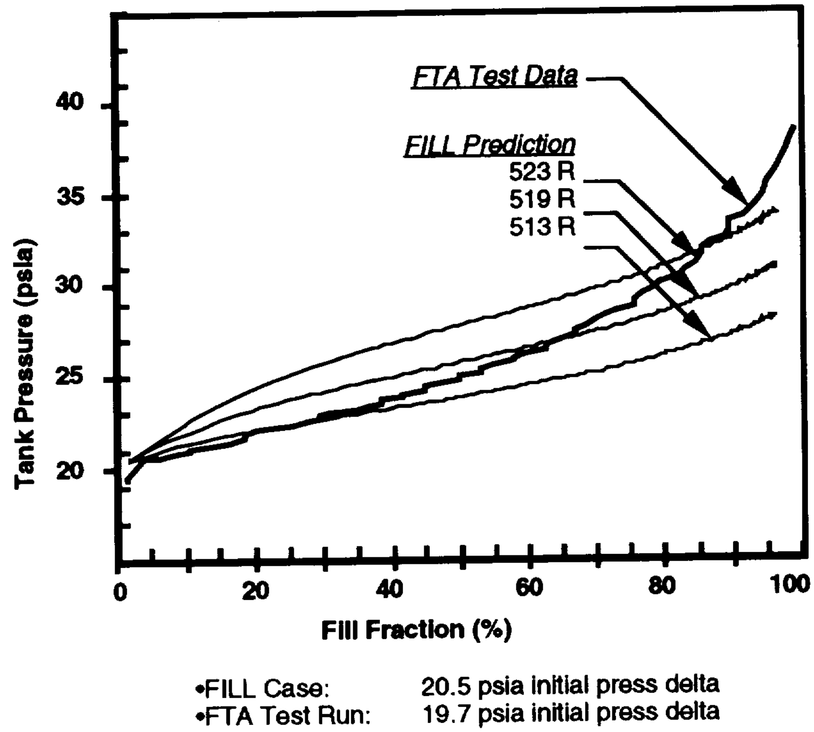

Figure 13. Variation of liquid inflow temperature.

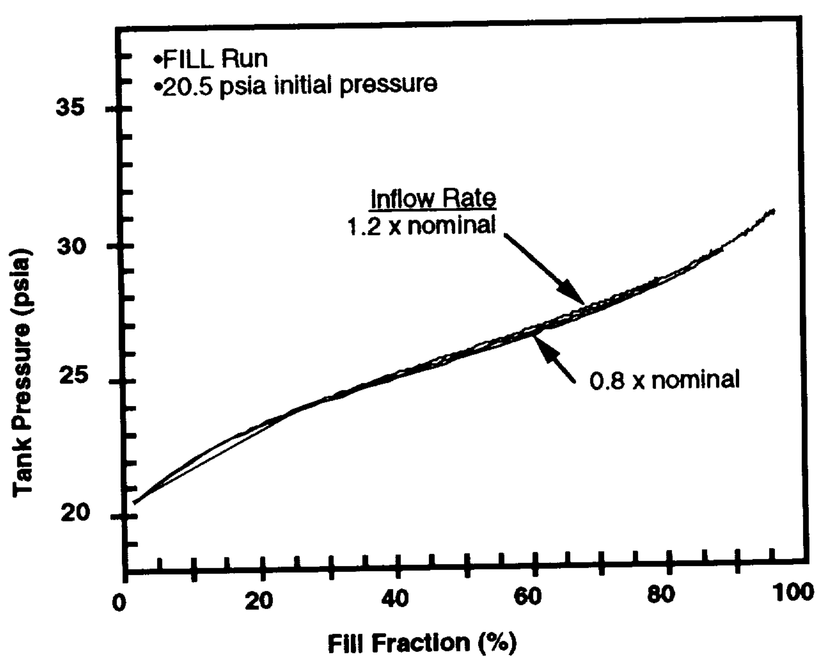

Figure 14. Variation of liquid inflow rate.

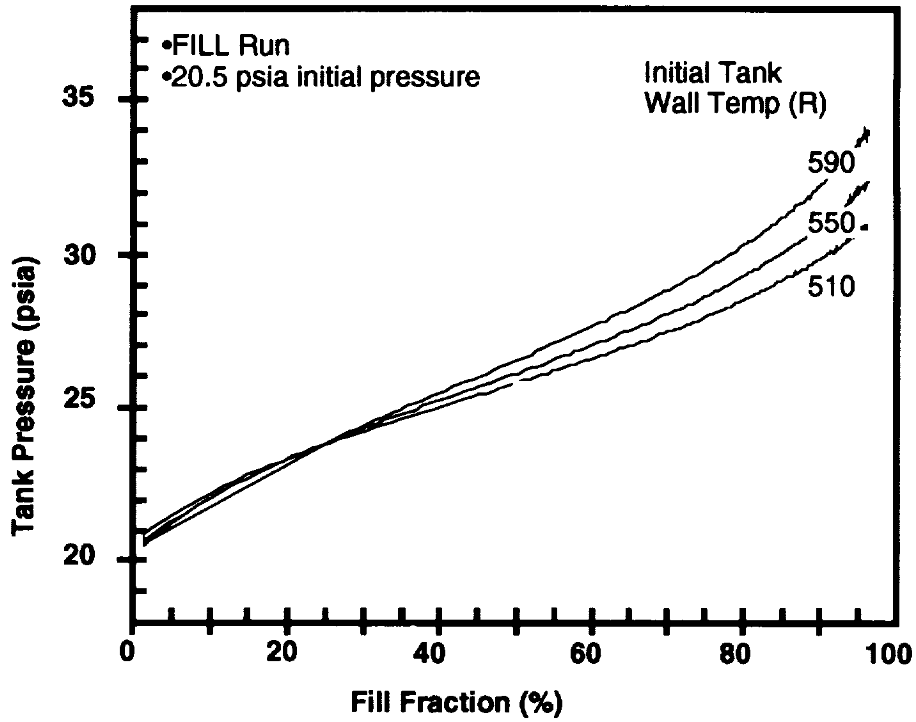

Figure 15. Variation of initial wall temperature.

A comparison between test data (fig. 11) and model predictions (figs. 12 through 15) indicates that the measured pressure fell within the range of test uncertainty. To better understand the difference between model and experiment behavior, FILL mass and energy relationships were evaluated by comparing derived gas and liquid temperatures with measured values. This was done by reversing the FILL program logic and iteratively solving for condensation rate at each time step. The iteration was driven by the convergence goal of matching the calculated pressure to within 0.05 psi of the measured value at each time step.

Figure 16 shows such a comparison between calculated and measured values of gas and liquid temperature. The plot portrays the results from an FTA test in which the average flowrate and inlet temperature were held at 13.0 g/m and 518 R, respectively. A comparison between the actual and predicted trace indicates a very good correlation throughout the entire fill process and further substantiates the FILL program's mass and energy relationships.

Evaluation of Condensation Theory

The final part of the analysis focused on deriving empirical/analytical equations for condensation rate for the two quiessant regimes.[10] Note that the active mixing regimes were not considered since their results pertain to a plumbing design inconsistent with practical applications. As stated before, the purpose was to improve transient mass transfer estimates in the FILL model and provide a fundamental basis for comparing two entirely different fill modes.

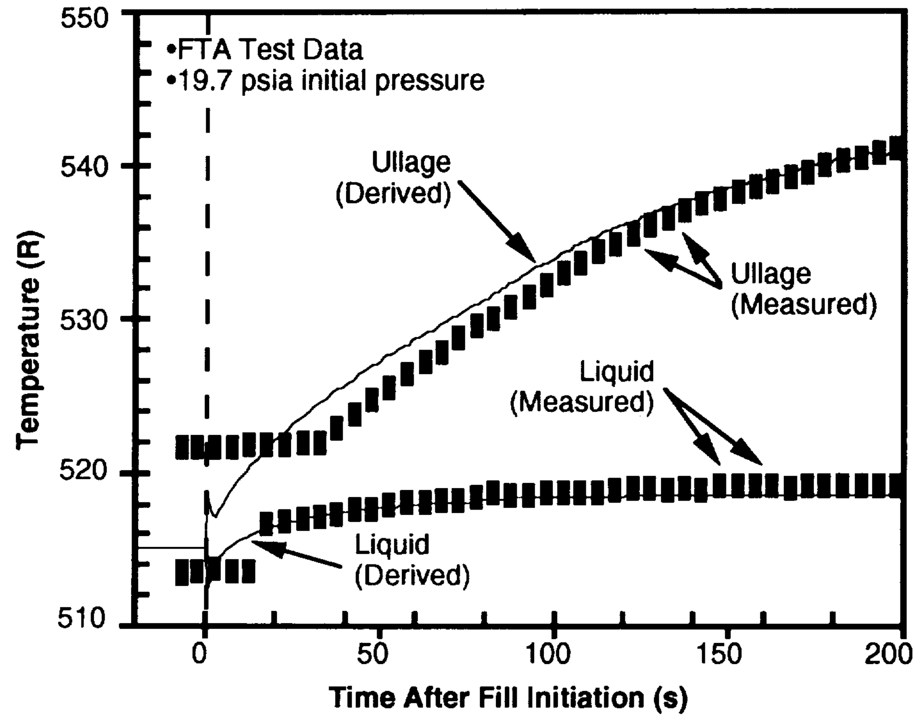

Figure 16. Tank fluid temperature versus time.

The condensation rate equation for each regime is expressed in terms of fluid thermodynamic properties, inflow rate, liquid level, jet characteristics, and tank geometry. An important aspect of this formulation is the representation of exposed liquid surface area. Another is the correlation for condensation flux obtained from universal submerged jet theory and test data. Although the equations for each regime are quite different in terms of functional trends, the forms are very similar. This enables the equations to be recast as a ratio indicative of relative condensation performance. By applying several simplifying assumptions, this ratio reduces to a function of nondimensionalized liquid level and top fill nozzle characteristics.

An interfacial turbulence/condensation flux model for the bottom fill regime was determined by inputing transient measurements of receiver tank pressure, temperature, and inflow rate from several bottom fill tests into the FILL model. The program's solution logic was reversed to enable back-calculation of condensation rate from the incorporated surface area algorithm and experimental pressures, temperatures, and inflow rate. The next step entailed expressing condensation rate in terms of a dimensionless condensation parameter, $StPr^{0.33}$, and representing time dependent fill levels as discrete values of z/D. The relationship between the condensation parameter and z/D is shown in figure 17. A least-squares linear curve fit of the data yields:

$$StPr^{0.33} = 0.062 - 0.017(z/D) \ . \tag{1}$$

At low z/D the actual rate is slightly higher than theoretically expected behavior. In this range, the tank is only partially filled and susceptible to breakup of the liquid surface. This results in an increase in the exposed surface area and higher-than-predicted condensation rates. Thomas[11] observed similar behavior in an experiment that examined low values of z/D for axial jets.

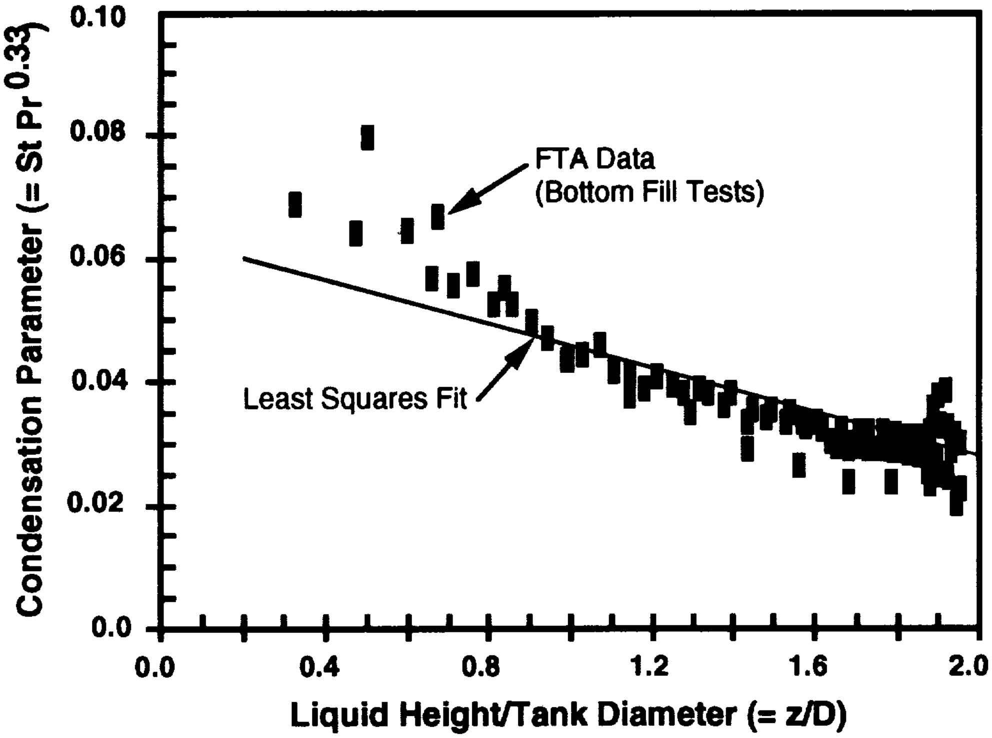

Figure 17. Turbulence/condensation model for submerged horizontal jet.

This effect is compounded by the horizontal jet orientation in the FTA receiver tank which enhances breakup during the initial phases of the fill process. Jet orientation is one of the major factors accounting for differences between derived values of condensation rate and predictions from the universal submerged jet model which are based on an axial jet orientation. This is also evident when examining flow regimes where $z/D \geq 1.0$. In this range, the derived condensation rates are slightly less than theoretical values. The horizontal jet orientation results in reduced surface turbulence and lower levels of condensation.

The top fill regime was similarly analyzed by modifying the surface area algorithm in FILL to model a downward-pointing, conical jet impinging on a steadily rising liquid surface (fig. 18). As before, values of condensation flux expressed in terms of *St* and *Pr* were paired against corresponding, time-dependent values of z/D. Figure 19 shows that this data are linear up to a z/D of approximately 1.7, which corresponds to a fill level of roughly 85 percent. For fill levels above this point, the rate tends to decrease in a nonlinear manner. A plausible explanation for this phenomenon is that as separation distance between the jet exit and surface decreases, disturbances caused by jet impingement into the bulk liquid are confined to a smaller area (i.e., much less than the total cross-sectional area). With deeper jet penetration, turbulence is confined to a smaller region and does not spread out over the entire liquid surface. Over the data's linear range (i.e., $0.0 \leq z/D \leq 1.7$), a least squares curve fit yields the following expression for $StPr^{0.33}$:

$$StPr^{0.33} = 0.082+0.082(z/D) \ . \qquad (2)$$

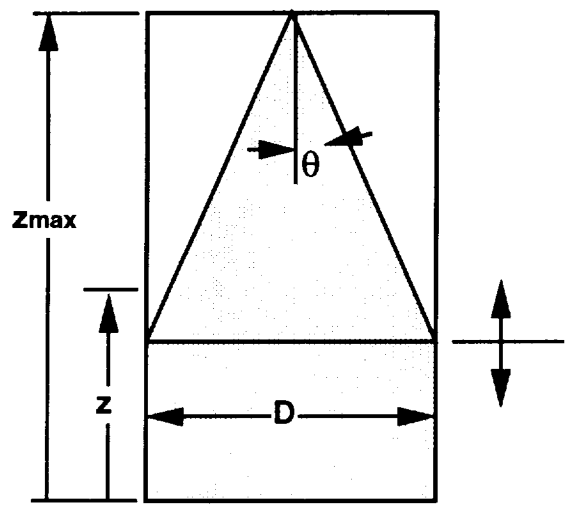

Figure 18. Revised surface area geometry—top fill.

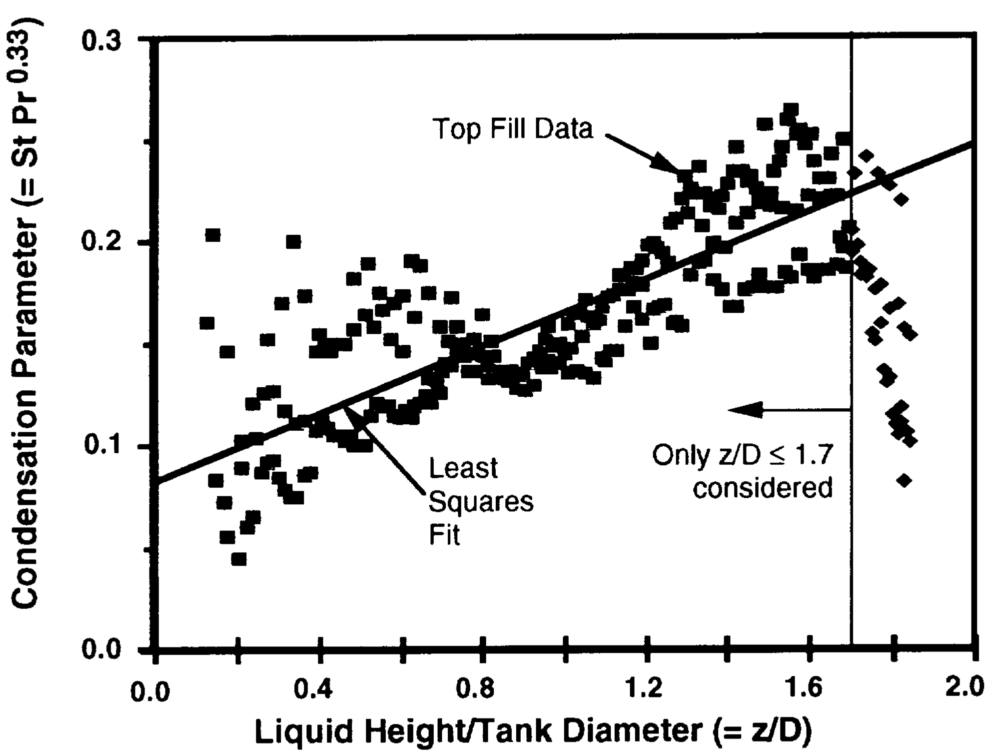

Figure 19. Turbulence/condensation model for quiessant top fill.

A final expression for condensation rate was derived by substituting the nondimensionalized condensation relationships (equations (1) and (2)) and appropriate surface area models into the following equation based on universal submerged jet theory.[8]

$$\dot{m}_{con} = \frac{C_l \Delta T \dot{m}_l}{H_{fg} D d} A_{con} \left(St Pr^{0.33} \right) . \tag{3}$$

A parameter indicative of relative performance was formulated by ratioing the expressions for condensation rate for the bottom fill and enhanced fill processes.

$$f_{con} = \frac{\dot{m}_{con}(z/D)_{\text{top}}}{\dot{m}_{con}(z/D)_{\text{bottom}}} \ . \tag{4}$$

This expression relates condensation of the enhanced top fill regime to that of the bottom fill regime, and includes terms for thermodynamic state, inflow rate, jet exit diameter and tank diameter. By assuming the same thermodynamic conditions, tank geometry and inflow characteristics, equation (4) reduces to two equations. For liquid heights in which the jet impinges on the tank sidewall (i.e., $0 \le z/D \le z/D_{\max} - ctn\,\theta$):

$$f_{con} = (sec\,\theta)\,\frac{0.082+0.082(z/D)}{0.062-0.017(z/D)} \ . \tag{5}$$

Alternatively, for levels in which the sides of the top fill jet intersects the horizontal liquid surface (i.e., $z/D_{\max} - ctn\,\theta < z/D \le z/D)_{\max}$):

$$f_{con} = \left[4\tan\theta\,(sec\,\theta - \tan\theta)(z/D_{\max} - z/D)^2 + 1\right]\frac{0.082+0.082(z/D)}{0.062-0.017(z/D)} \ . \tag{6}$$

Figure 20 shows the variation of f_{con} with dimensionless liquid level for different values of inlet jet half angle. This plot illustrates the enhanced regime's consistently higher condensation rates over the range of liquid levels. The valid range ($0 \le z/D \le 1.7$) is limited to that considered in the linearized surface turbulence correlation for condensation flux. The upper bound of this range is denoted by the so-called turbulence limit. Note that the convergence of f_{con} to a singular value at $z/D_{\max}$ does not reflect expected behavior at high z/D. Above the turbulence limit, f_{con} should drop off severely, in a manner similar to the condensation parameter in figure 19. In addition the turbulent limit is probably half-angle dependent. Although this aspect was not investigated experimentally, it is anticipated that narrowing the jet half-angle will reduce the liquid level at which turbulent spreading becomes suppressed. Therefore, the dropoff point or turbulence limit should increase with larger jet half-angles.

Figure 20 also illustrates the change in enhanced fill condensation behavior (i.e., functional relationship between condensation rate and z/D) as liquid passes the jet impingement limit. For z/D less than this transition, f_{con} follows the relationship in equation (5). For values above this point, the exposed area for the top fill process becomes more sensitive to z/D (equation (6)) and decreases with liquid height. This indicates that there is a maximum value of condensation rate driven by physical interaction of the jet with the tank wall. As a consequence, f_{con} is constrained by a maximum value that depends on the jet half-angle. Over a range of half-angles of 15 to 45° the maximum condensation rate for the enhanced technique varies from 5 to 8 times that of the bottom fill technique.

The functional relationship for f_{con} indicates that condensation rate for the enhanced fill process will always be greater than that for passive bottom fill, at least over the range of the interfacial turbulence linearization ($z/D \le 1.7$). It also suggests increased ullage collapse and lower pressure rise rates for the enhanced process.

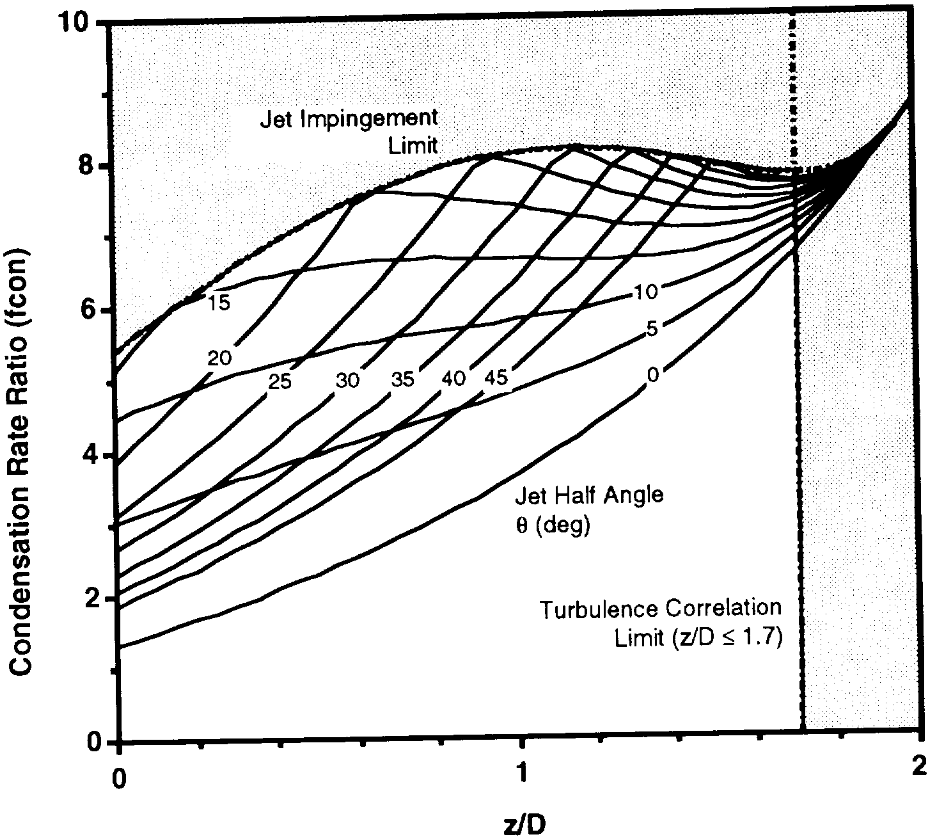

Figure 20. Comparison between top and bottom fill condensation behavior.

CONCLUSIONS

An experimental and analytical investigation of performance for various no-vent fill techniques has been completed using Freon-114. The major conclusions drawn from the investigation include:

1) The quiessant top fill represents the most effective technique in terms of improving performance and reducing hardware complexity. Transfers employing this method typically resulted in fill times 20- to 50-percent lower than comparable passive bottom fill tests. The performance improvements were most likely due to the increased agitation caused by liquid impinging on the liquid surface. These results were further supported by empirically derived equations which relate condensation behavior between the two processes. The substantial improvements associated with top fill suggest that a simple inlet/jet design may suffice for many applications, particularly in "settled fill" concepts where the inflow nozzle is positioned above the liquid surface. Also, the results emphasize the importance of mixing for "unsettled fill" approaches.

2) Test measurements of pressure, temperature and fill level correlate well with the transient behavior predicted by the FILL pressurization model. This has increased confidence in the model's algorithms and validated the program's use for future ground tests. The validation also provides a solid starting point for inclusion of algorithms accounting for liquid surface behavior/orientation under low-gravity.

3) Experimental data appears to correlate well with condensation models based on universal submerged jet theory. This particularly held true for the bottom fill which was easiest to characterize in terms of surface area. The investigation also demonstrated extension of submerged jet theory to cases of off-axis jet orientations and enhanced fill regimes. This represents a convenient approach for modeling mass transfer in no-vent fill computations.

Results pertaining to active mixing were not as definitive due to the circulation loop's restrictive design. However, there were indications that this type of regime improved performance at higher pressure ratios regardless of the circulation plumbing arrangement.

The test program also yielded valuable insights and "lessons learned" applicable to design of ground tests, small-scale flight experiments and future spaceflight systems. One observation was the extreme sensitivity of transfer tank (T2) pressure to state within the fluid lines and equipment when employing autogenous pressurization. Another was the control complications caused by condensation and evaporation in test article lines and plumbing.

Future efforts in this area will likely focus on large-scale cryogenic ground tests and small-scale flight experiments with either cryogens or cryogen simulants. However, small-scale non-cryogenic experiments, such as the FTA, can still yield valuable data and serve as a precursor for more expensive and complex cryogenic experimentation.

Due to the simplicity of Freon testing (relative to that with cryogens), a wide range of test conditions and hardware configurations can be rapidly performed at low cost to establish performance trends and sensitivities. For instance, the analysis involving turbulence/condensation models pointed to many issues that would be best addressed using this approach. Possible activities include examination of different tank height/diameter ratios and nozzle flow arrangements, and investigations of atomization on a system-scale. Any future experiments, however, should be conducted in a controlled environment to improve control of thermodynamic state and eliminate susceptibility to ambient conditions. In addition, use of transparent receiver tanks should be considered in order to provide a better understanding of mixing processes and flow patterns within the tank.

REFERENCES

1. Chato, D.: "Analysis of the Nonvented Fill of a 4.96-Cubic-Meter Lightweight Liquid Hydrogen Tank." NASA Tech Memo 102039, August 1989.

2. Chato, D.: "Thermodynamic Modeling of the No-Vent Fill Methodology for Transferring Cryogens in Low Gravity." NASA Tech Memo 100932, AIAA Paper 88-3403, 1988.

3. DeFelice, D., and Aydelott, J.: "Thermodynamic Analysis and Subscale Modeling of Space-Based Orbit Transfer Vehicle Cryogenic Propellant Resupply." NASA Tech Memo 89921, AIAA Paper 87-1764, 1987.

4. Gille, J.: "Analysis and Modeling of Fluid Transfer in Orbit." AIAA Paper 86-1718, 1986.

5. Vaughan, D., and Schmidt, G.: "Analytical Modeling of No-Vent Fill Process." AIAA Paper 90-2377, 1990. To be published in AIAA J. Spacecraft and Rockets.

6. Moran, M., Nyland, T., and Papell, S.: "Liquid Transfer Cryogenic Test Facility-Initial Hydrogen and Nitrogen No-Vent Fill Data." NASA Tech Memo 102572, March 1990.

7. Jones, O., Meserole, J., Hedges, D., and Schmidt, G.: "Conceptual Design of the Subscale Orbital Fluid Transfer Experiment (SOFTE)." AIAA Paper 90-2378, 1990.

8. Hemlick, M., Khoo, B., Brown, J., and Sonin, A.: "Vapor Condensation Rate at a Turbulent Liquid Interface, for Application to Cryogenic Hydrogen." AIAA Paper 88-0559, 1988.

9. Brown, J., Hemlick, M., and Sonin, A.: "Vapor Condensation at a Turbulent Liquid Surface in Systems with Possible Space-Based Applications." AIAA Paper 89-2846, 1989.

10. Vaughan, D., Faust, D., and Schmidt, G.: "Enhancement of the No-Vent Fill Process." AIAA Paper 91-1842, 1991. Submitted for publication in AIAA J. Spacecraft and Rockets.

11. Thomas, R.: "Condensation of Steam on Water in Turbulent Motion." Int. J. Multiphase Flow, vol. 5, 1979, pp 1–15.

APPROVAL

NO-VENT FILL PRESSURIZATION TESTS USING A CRYOGEN SIMULANT

By G.R. Schmidt, R.W. Carrigan, J.E. Hahs, D.A. Vaughan, and D.C. Foust

The information in this report has been reviewed for technical content. Review of any information concerning Department of Defense or nuclear energy activities or programs has been made by the MSFC Security Classification Officer. This report, in its entirety, has been determined to be unclassified.

J.P. MCCARTY
Director, Propulsion Laboratory

☆ U.S. GOVERNMENT PRINTING OFFICE 1992—631—060/60012